Spatial Dynamics of Phymatotrichum Root Rot in Row Crops in the Blackland Region of North Central Texas

M. J. Jeger, C. M. Kenerley, T. J. Gerik, and D. O. Koch

First, second, and fourth authors, Department of Plant Pathology and Microbiology, Texas Agricultural Experiment Station, The Texas A&M University System, College Station 77843; third author, Blackland Research Center, Texas Agricultural Experiment Station, Temple 76501. Present address of first author: Tropical Development and Research Institute, London, WC1X 8LU, UK.
Accepted for publication 11 May 1987 (submitted for electronic processing).

ABSTRACT

Jeger, M. J., Kenerley, C. M., Gerik, T. J., and Koch, D. O. 1987. Spatial dynamics of Phymatotrichum root rot in row crops in the Blackland region of north central Texas. Phytopathology 77:1647-1656.

The spatial dynamics of Phymatotrichum root rot were mapped in field plots of cotton and soybean at Temple and cotton only at Brandon in the Blackland region of north central Texas in 1984. First symptoms of Phymatotrichum root rot were observed in mid-June, and assessments were made until mid-August. Analysis of the spatial dynamics indicated that the expansion of runs (sequences of diseased plants within rows) was a major component of increase. The spatial patterns of increase were consistent with plant-to-plant spread by hyphal strands in addition to a time-dependent symptom expression corresponding to an underlying distribution of sclerotia. Various analyses were used to describe and quantify the spatial patterns and dynamics of Phymatotrichum root rot. Spatial autocorrelation analyses were used to test the hypotheses of nonrandom spatial patterns of diseased plants within and across rows. The patterns observed indicated that plant-to-plant spread within rows was more important than spread across rows. The influence of neighboring 1-m row segments of plants, both contiguous (within rows) and adjacent (across rows), was evaluated by calculating the relative frequencies that a disease-free segment contained at least one diseased plant after a 7-day interval. A linear regression model was derived to predict the relative frequency of transition in terms of the status (diseased or healthy) of its nearest neighbors. The regression coefficients indicated that the influence of contiguous neighbors was more important than that of adjacent neighbors. The relative frequencies that a run of a given length class extended to a longer class during a 7-day interval were calculated and found to be inversely related to the difference in length between length classes.

Additional key words: *Phymatotrichum omnivorum,* root disease, spatial analysis.

Phymatotrichum omnivorum (Shear) Duggar (*Phymatotrichopsis omnivora* (Duggar) Hennebert) causes root rot in many crops in the southwestern United States and northern Mexico (29,53). The pathogen has a very restricted geographical distribution (44) limited to this region of the world. The disease incited, Phymatotrichum root rot, is a major constraint on cotton (*Gossypium hirsutum* L.) production in areas such as the Blackland region of north central Texas, where soil types (alkaline clays) are especially conducive to the pathogen (49,54). In years when precipitation and soil moisture are high during the early summer months, the disease is responsible for almost 100% crop mortality in fields where the pathogen is present (21). A major limitation in current pest management programs (11) is that integrated pest management (IPM) decisions are made without information on the incidence and effects of Phymatotrichum root rot on lint yield. Currently, no chemical treatments are available for Phymatotrichum root rot, and there are no economic cultural practices that can be routinely used to control the disease. There has been a decline in cotton production in the Blackland region (3), and Phymatotrichum root rot has often, if anecdotally, been cited as a major contributing factor.

The life cycle of Phymatotrichum root rot is reasonably well characterized (29,53). The fungus perennates as sclerotia or as hyphal strands formed in previous years (1,2,27,40). Early in the growing season, when soil temperatures have risen sufficiently, sclerotia germinate and form new strands, and these make contact with developing root systems of host plants. Strands typically grow ectotrophically to the crown, almost exclusively on the taproot in cotton, before penetrating and killing the plant. Most evidence supports the view that root contact (29,53) is not necessary for plant-to-plant spread (10,26,29) and that growth through soil occurs in advance of the region of diseased roots.

Recently, Jeger and Lyda (21) analyzed historical data on epidemics of Phymatotrichum root rot to evaluate the feasibility of developing a forecasting scheme in cotton. A missing ingredient from the forecasting scheme, at present, is detailed information on the spatial dynamics of Phymatotrichum root rot as the disease develops from initial foci of infection to the high incidences obtained when environmental conditions are favorable. The pathogen can grow through soil from infected to healthy plants, but the relative contribution to disease dynamics, compared with infection by spatially distributed sclerotia in the soil, has not been investigated.

Early workers emphasized the spatial patterns of disease increase in cotton and produced maps demonstrating these patterns (23–26,37–39,48,50). These maps emphasized the radial expansion of Phymatotrichum root rot centers over a number of growing seasons (22,25,37–39) and also the within-season increases by means of the formation of runs (sequences of diseased plants) within rows of cotton. The maps were presented largely without quantitative analysis or interpretation, and often, within-season assessments were not made frequently enough to analyze the spatial development of disease. Similar maps have been prepared for other root and foliar diseases (8,9,15,31,47,58), but again, there have been few analyses of the underlying mechanisms generating these patterns. Some interpretation of the spatial dynamics of disease has occasionally been made for soilborne pathogens (7,9,12,17,46).

Techniques for examining the spatial patterns of pathogen propagules in the soil have been proposed, compared, and critiqued (5,6,43). Similarly, techniques for examining the patterns of diseased plants (33,34,36,52) have been evaluated. Occasionally, the two types of pattern have been related (9,51). Valuable as these studies have been, they suffer from the defect that they are essentially static; samples are taken on one occasion and statistical distributions are tested for goodness of fit to the observed pattern. There is an urgent requirement for quantitative techniques to analyze spatial patterns of disease developing in time in crops of varying geometries, e.g., row crops. To our knowledge, techniques are not fully available for this purpose. The main purpose of the study described in this paper was to evaluate the spatial dynamics of Phymatotrichum root rot with various mapping, statistical, and other quantitative techniques.

MATERIALS AND METHODS

Two sites in the Blackland region of north central Texas were used for monitoring Phymatotrichum root rot epidemics in 1984: a commercial farm at Brandon, 16 km east of Hillsboro, and experimental plots at the Blackland Research Center, Temple. The soil at each site was classified as a Houston black clay (Udic Pellusterts [fine, montmorrillonitic, thermic]). Both sites had been planted to cotton for at least 60 yr. The symptoms used in disease assessments were the initial wilting of upper leaves followed rapidly by wilting of the lower leaves and plant death (53). Plants showing the first symptoms of bronzing of leaves were not recorded as diseased. In practice, the extremely rapid symptom development and the raised leaf temperature during wilting gave unambiguous symptom expression and few assessment errors.

Brandon site. An area in a commercial cotton field was assessed for root rot in early June 1984. The field had been treated with 67 kg N/ha preplant and planted with cultivar Lankart 611 on 15 April 1984. Postemergence density in early June was 87,000 plants per hectare. The first appearance of plants with symptoms of root rot was noted on 12 June. The field was sprayed according to conventional farm practices for weeds and insect pests throughout the season.

An area comprising 56 rows (0.9-m row spacing × 120 m/row), situated in a disease-prone area, was selected from aerial photographs of disease progress taken in previous years and was marked out to encompass the initially diseased plants. The position of each diseased plant was marked with a wire flag, and the distance from a standard reference line marked at right angles to the rows was measured with a hand-held tape. The area assessed was subsequently limited to a contiguous area of 32 rows × 80 m/row and was assessed by walking each row on 19 and 26 June, 3, 10, 17, and 31 July, and 7 August. All assessments were made in a period of 4 hr and were completed before noon on each occasion.

On each assessment date, the appearance of newly diseased plants was marked with wire flags, and their position was measured with respect to the standard reference line. Where an uninterrupted sequence (run) of diseased plants was present, only the plants at the extreme positions were flagged and measured; the number of plants in the run was counted. Occasionally, plants that did not enter the reproductive phase were encountered; these plants were ignored in making counts. Flags of different colors were used on each pair of sampling occasions to facilitate the assessment of newly diseased plants. A leaf desiccant was applied in mid-August to facilitate harvest, precluding further assessment of Phymatotrichum root rot.

Temple site. A rectangular area 180 × 75 m (108 rows 0.7 m apart) was planted to cotton (cultivar GP3774) and soybean (*Glycine max* L. cv. Dowling) on 17 April 1984 with about 75,000 plants per hectare. The area was sown as four plots (each 54 rows × 85 m/row) with cotton and soybean at opposing positions in the rectangle. The planting date was followed by a dry period that delayed and reduced emergence of both cotton and soybean. Crop phenology, as a consequence, was behind that at Brandon. Plants showing symptoms of Phymatotrichum root rot were first noted in both crops on 19 June; the positions of the initially diseased plants were marked with wire flags and measured with respect to a standard reference line at right angles to the rows. One subplot within each of the four plots (21 rows × 20 m/row and 22 rows × 30 m/row in soybean; 24 rows × 30 m/row and 21 rows × 20 m/row in cotton) was subsequently marked out to encompass the initially diseased plants and used for subsequent assessments. Disease assessments were made on 19 and 26 June, 2, 12, 18, and 30 July, and 13 August by the same procedure described for Brandon. The plots were cultivated and hand-weeded for weed control and sprayed according to the normal station programs for pests.

Analysis of spatial pattern. Statistical and other quantitative techniques were used to analyze the spatial patterns of Phymatotrichum root rot at the Brandon and Temple sites. These included ordinary runs analysis, spatial autocorrelation, nearest neighbor analysis, and analysis of the dynamics of run expansion.

Ordinary runs analysis is a one-dimensional form of spatial autocorrelation; it is especially suited for detecting nonrandom patterns of diseased plants within rows of plants (34,35), whether caused by clumping of inoculum in the soil or by plant-to-plant increase of the disease (5). The one-dimensional nature of the analysis arises from the practice of joining adjacent rows to form one continuous row. Application of the analysis at Brandon indicated a nonrandom (clumped) pattern of diseased plants within rows at the second assessment on 19 June; this finding was confirmed throughout the remaining assessments. The analysis could not be used to assess nonrandom patterns across rows because of the nonlattice planting pattern of cotton. Accordingly, an abstract lattice, comprising two symbols, 0 and 1, was prepared by making transects across the rows at 1-m intervals; the value 1 was entered if the transect crossed a sequence of diseased plants in a row, and the value 0 if the transect crossed a sequence of healthy plants. Thus, an $m \times n$ matrix was obtained in which m was the number of rows and n the number of transects across rows. Ordinary runs analyses were made along transects (across rows) and within rows. Failure to reject randomness along transects (across rows) but rejection of randomness within rows was taken to indicate that patterns of diseased plants were due, predominantly, to plant-to-plant spread within rows.

A more thorough analysis of the pattern of diseased plants was made using spatial autocorrelation. Again, because of the nonlattice crop geometry, it was necessary to derive an abstract pattern of symbols from the raw data. Rows were divided into 1-m segments, and a zero was entered if there was no diseased plant in the segment or a 1 was entered if there was at least one diseased plant in the segment. The general cross-product statistic, r (56), was used to examine the spatial autocorrelation present in the data. The statistic is based on two matrices, W and Y; the W matrix defines the spatial proximity of locations, and the Y matrix represents a measure of proximity. The statistic has the advantage that spatial proximity can be defined in various ways and used to differentiate, in our case, between contiguous and adjacent segments. Thus, spatial pattern within rows (contiguous) and across rows (adjacent) can be examined separately by different specifications of the matrix W. A program to compute the statistic was written in the programming language PL/I.

Nearest neighbor analysis. The spatio-temporal attributes of the Phymatotrichum root rot epidemics were examined further by examining the relationship between the status of neighboring 1-m segments (with entries 0 or 1 as for the spatial autocorrelation analysis) and the relative frequency a segment made the transition from 0 (healthy) to 1 (diseased) during a 7-day interval. Because of the irregular sampling interval at Temple, only Brandon data were used in these analyses. At each sampling, each healthy segment with the exception of those on the boundary of the sampled area was coded to indicate the configuration of surrounding segments. Adjoining segments within the same row were termed, as before, contiguous segments; neighboring segments across rows were termed adjacent segments. Because each healthy segment can be surrounded by 0, 1, or 2 contiguous diseased segments and by 0, 1, or 2 adjacent diseased segments, nine configurations are possible for each healthy segment. The healthy segments in each of these nine classes were counted at each sampling; the relative frequency of transition from healthy (0) to diseased (1) during the following week was calculated for each class. In addition, the totals and the numbers making a given transition over all sampling occasions were summed separately, and relative frequencies for each of the nine classes were calculated for the whole assessment period.

A linear model, in which the relative frequencies (p) were transformed to logits to equalize variance at low and high values of p and regressed against independent variables x_1 (the number of contiguous diseased segments) and x_2 (the number of adjacent diseased segments), was evaluated:

$$\ln [p/(1-p)] = a_0 + a_1x_1 + a_2x_2 + e, \quad (1)$$

where a_0 is the predicted value of logit (p) when x_1 and x_2 are 0, a_1 and a_2 are regression coefficients, the magnitudes of which represent the relative importance of within-row (a_1) compared with

across-row (a_2) spread, and e represents random error on a logit scale. This model was fitted to the relative frequency data for each occasion separately and for the combined data; in each case, regressions were based on eight degrees of freedom. Because relative frequencies are a binary proportion, they were weighted by their respective denominators in the regressions. A further model was fitted with time (t) explicitly accounted for:

$$\ln [p/(1-p)] = a_0 + \beta t + a_1 x_1 + a_2 x_2 + e. \quad (2)$$

This model was fitted for all data to give a regression equation based on 43 degrees of freedom. The importance of including time was then assessed by omitting the t term and repeating the analysis, again with 43 degrees of freedom.

With the exception of one time period (17 July through 7 August), all assessments at Brandon were made at weekly intervals. Because of the completeness of the assessments, it was possible to tabulate the progress of each run observed from first appearance to eventual merging with other runs. A detailed analysis was made of the frequencies with which runs in one length class (z_1) made the transition to another length class (z_2) during each weekly period (i.e., excluding the 17 July through 7 August changes). Length classes of 1.5-m intervals were chosen (about 2% of row length); the number of transitions for all permissible pairs of length classes ($z_2 \geqslant z_1$) for each time period was calculated and converted to a relative frequency by dividing by the total number of transitions from the initial length class.

RESULTS

Spatial patterns at Brandon. The patterns of Phymatotrichum root rot incidence on the eight assessment dates are shown in Figure 1 as complete spatial maps. On 12 June, there were a few plants diseased within the area surveyed. One week later, on 19 June, there had been a considerable increase in Phymatotrichum root rot with runs becoming evident. The formation of runs became more pronounced throughout June and July. By the last assessment on 7 August, before desiccation of the cotton, 55% of the total length of rows of cotton in the surveyed rows was occupied by plants killed by Phymatotrichum root rot. Key statistics of spatial dynamics were derived from these data (Fig. 2).

The total number of diseased plants increased sigmoidly in the assessed area and leveled off at about 10,000 plants in early August (Fig. 2A). The number of runs increased rapidly in June but leveled off in early July and then decreased because of the merging of runs (Fig. 2B). The mean number of diseased plants per run increased linearly throughout most of the assessment period (Fig. 2C). The distribution of the mean number of dead plants per run was, however, highly skewed. On 19 June, about 97% of all runs had fewer than 10 diseased plants per run (a mean of about three), and no run was longer than 20 plants. On 7 August, most runs (about 85%) had fewer than 50 diseased plants per run (Fig. 2D), but there were many runs of greater size. The mean number of diseased plants per run was about 13, and several runs had more than 100 diseased plants. The results for mean length of run and the

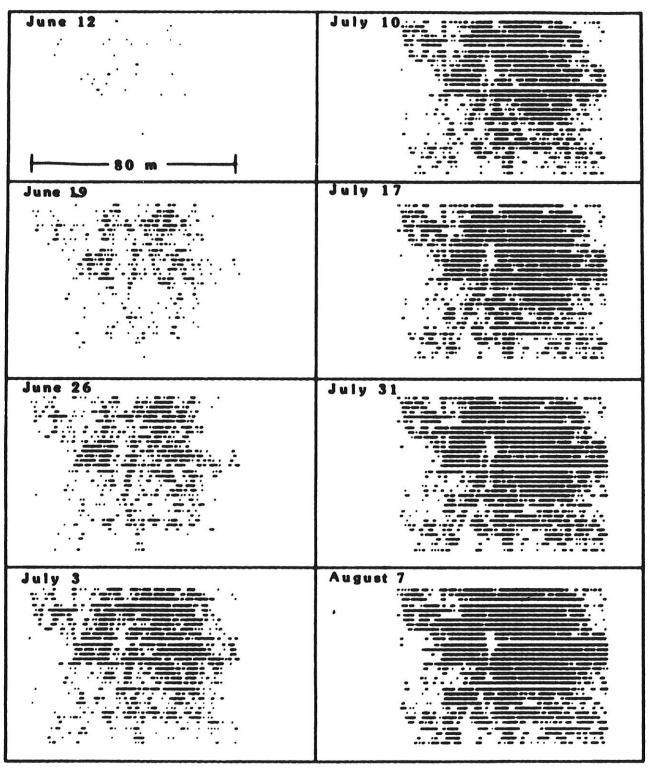

Fig. 1. Spatial patterns of Phymatotrichum root rot incidence in cotton on eight assessment dates at Brandon, TX. Assessment area was 32 rows × 80 m/row. Sequences (runs) of diseased plants are represented (within the limits of resolution) by continuous lines.

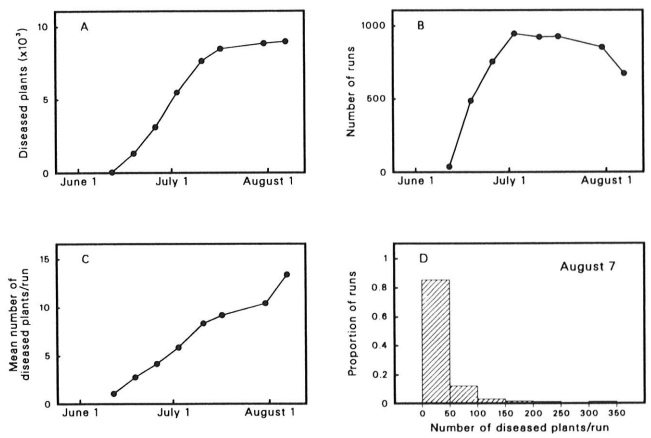

Fig. 2. A, Total number of diseased plants, **B,** number of runs (sequences of diseased plants), **C,** mean number of diseased plants per run on eight assessment dates, and **D,** frequency distribution of number of diseased plants per run at the last assessment date at Brandon in cotton plots 32 rows × 80 m/row.

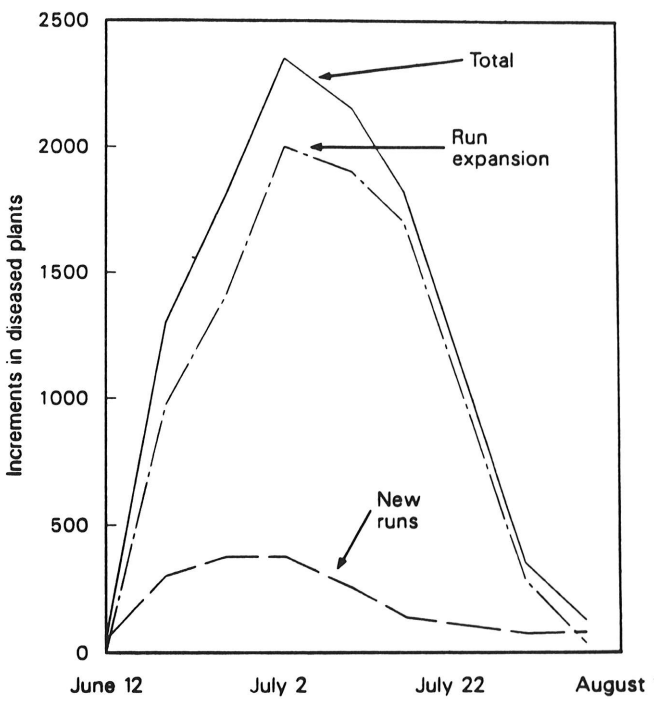

Fig. 3. Increments in number of diseased cotton plants at each assessment date at Brandon (——) partitioned into those due to run expansion (– · –) and those due to the formation of new runs (– – –).

distribution of length of run were similar to those for number of diseased plants and are not shown.

It was possible to differentiate between the increases in diseased plants that were contiguous with and thus gave expansion of existing runs and the increases in diseased plants that were not contiguous and thus gave new runs, where these comprised $n = 1, 2, 3 \ldots$ diseased plants. The increments in diseased plants, plotted in Figure 3, are partitioned into the increments due to run expansion and those due to new runs. By early July, the percentage due to new runs had dropped to less than 20% of the total increment. The data for the newly arisen runs are analyzed further in Figure 4. Most of the runs consisted of one or two diseased plants when first observed although an appreciable number contained three to seven diseased plants. The maximum number of diseased plants in a new run was 15.

Spatial patterns at Temple. The results of the assessments of Phymatotrichum root rot in soybean are shown in Figure 5A and B. On 19 June, there were few diseased plants in either plot. Runs did not become obvious until the third assessment (12 July) in plot A (Fig. 5A) and the last assessment (13 August) in plot B (Fig. 5B). By the last assessment on 13 August, 51 and 31%, respectively, of the total length of row in plots A and B was occupied by soybean plants killed by Phymatotrichum root rot.

The pattern of Phymatotrichum root rot incidence in cotton is shown in Figure 5C and D for each assessment date. On 19 June, there were few diseased plants in either plot. In plot A, runs had begun to form by 12 July, but it was not until the last assessment on 13 August that extensive mortality and run formation were apparent (Fig. 5C). In plot B, very few diseased plants were present until the last assessment (Fig. 5D). By the last assessment on 13 August, 36 and 15% of the plants in plots A and B, respectively, were diseased.

Because of the limited and later Phymatotrichum root rot development in plots B for both soybean (Fig. 5B) and cotton (Fig. 5D), statistics of spatial increase are only presented for plot A. The number of diseased soybean plants increased sigmoidly in plot A to about 550 plants in late July but then increased to about 700 in early August (Fig. 6A). The number of runs increased rapidly in June, leveled off in July, and was declining at the last assessment (Fig. 6B). The curve for the mean number of diseased plants per run (Fig. 6C) was of similar shape to that for total number of diseased plants (Fig. 6A). The distribution of the mean number of diseased plants per run at the last assessment (Fig. 6D) was similar to that at Brandon, although more evenly distributed (taking into account scale) because of the late appearance of runs on the last assessment. The patterns of increases in mean length of run were similar to those for mean numbers of diseased plants.

The number of diseased cotton plants and the number of runs were dominated by the late increase in Phymatotrichum root rot in early August (Fig. 7A,B). The mean number of diseased plants per run at this time (Fig. 7C) was about five in each plot; these runs, on average, were less than 1 m long. The distribution in number of diseased plants per run was skewed (Fig. 7D) but again more even due to the late increases as new runs on the last assessment. The pattern with length of run was again similar to number of diseased plants per run.

The pattern of newly arisen runs differed from that observed at Brandon; the number of newly arisen runs was low in both soybean and cotton plots in June and July but then increased markedly in August.

Ordinary runs analysis of spatial pattern. Different results were obtained at the two sites in this study (Table 1). At Temple, in cotton, it was not possible to reject randomness of diseased plants when considering across-row patterns in cotton until the last assessment $Z(U) > |-1.64|$; in soybean, randomness could not be rejected at any assessment. The hypothesis of random pattern within rows was rejected in both crops at a very early stage of the epidemic. At Brandon, random patterns were rejected across and within rows early in the epidemic; the number of observed runs was always lower within rows than across rows, indicating more marked clumping within rows.

Spatial autocorrelation. The results with spatial autocorrelation were essentially the same as those obtained using ordinary runs analysis, and typical results for cotton are shown in Table 2. In all cases, although random patterns were rejected both within and across rows, the observed value of r was almost always less for the contiguous configuration and randomness rejected sooner.

Nearest neighbor analysis. Results of the nearest neighbor analysis using equation 1 are given in Table 3. Two major trends were apparent from these data: first, the relative magnitude of the coefficients indicates that spread within rows was more important

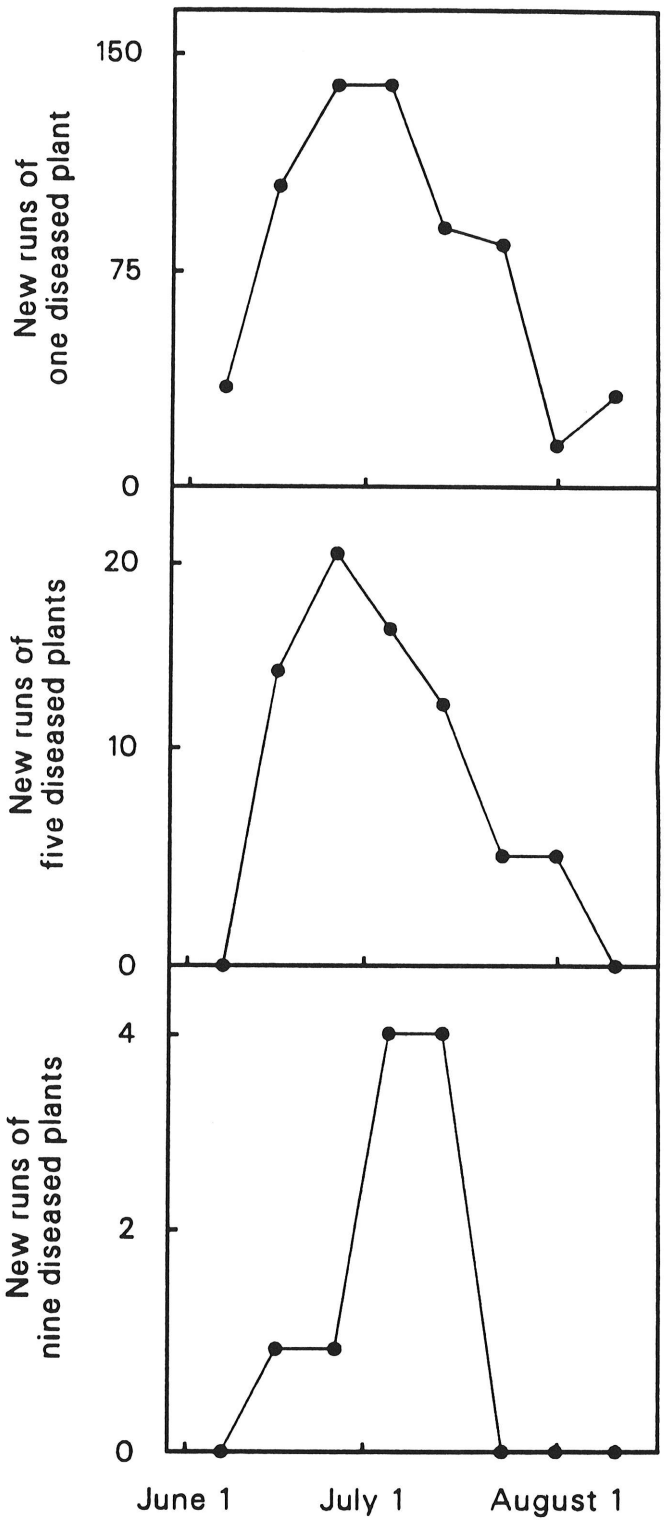

Fig. 4. Number of newly arisen runs containing (top to bottom) one, five, and nine diseased plants over eight assessment dates at Brandon in cotton plots 32 rows × 80 m/row.

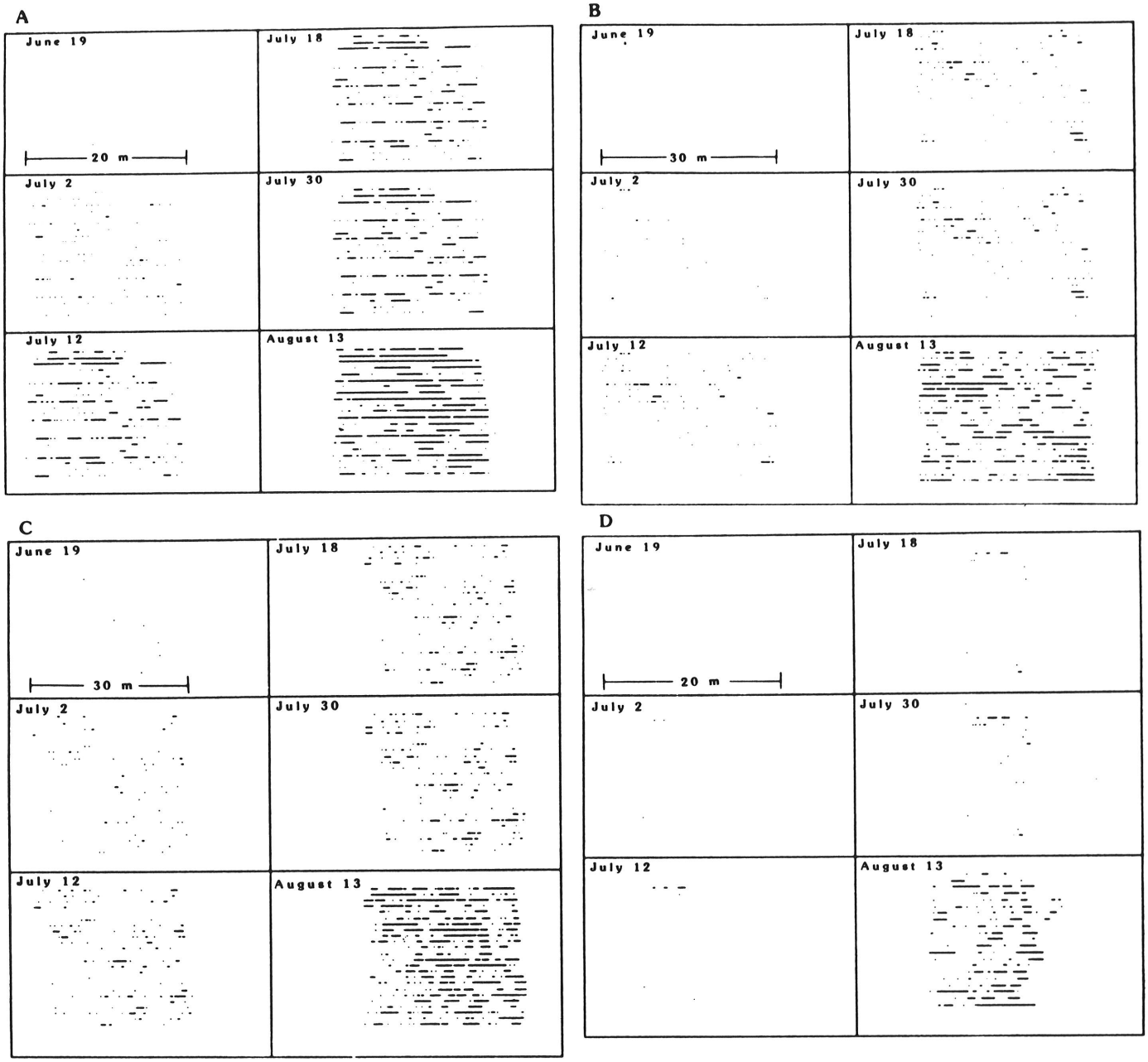

Fig. 5. Spatial patterns of Phymatotrichum root rot incidence in soybean and cotton on six assessment dates at Temple: **A,** soybean A, 21 rows × 20 m/row; **B,** soybean B, 22 rows × 30 m/row; **C,** cotton A, 24 rows × 30 m/row; and **D,** cotton B, 21 rows × 20 m/row (shown as bars at the first assessment date). Sequences (runs) of diseased plants are represented (within the limits of resolution) by continuous lines.

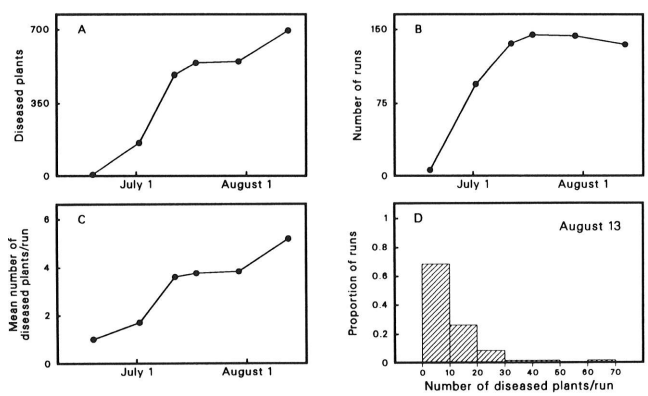

Fig. 6. A, Total number of diseased soybean plants, **B,** number of runs (sequences of diseased plants), **C,** mean number of diseased plants per run on six assessment dates, and **D,** frequency distribution of number of diseased plants per run at the last assessment date at Temple in soybean plot A, 21 rows × 20 m/row.

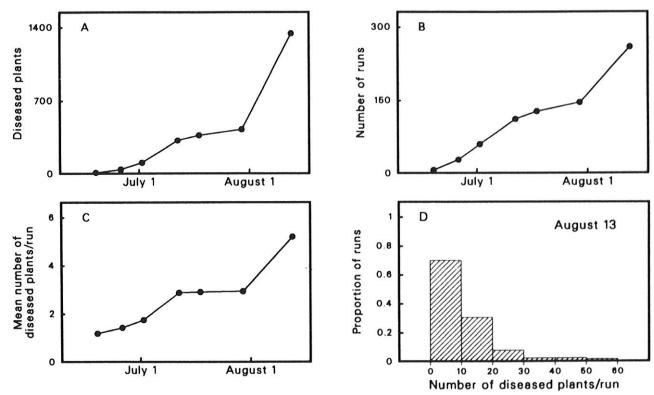

Fig. 7. A, Total number of diseased cotton plants, **B,** number of runs (sequence of diseased plants), **C,** mean number of diseased plants per run on six assessment dates, and **D,** frequency distribution of number of diseased plants per run at the last assessment date at Temple in cotton plot A, 24 rows × 30 m/row.

TABLE 1. Results of ordinary runs analysis of patterns of Phymatotrichum root rot in cotton and soybean at Temple and in cotton at Brandon, TX

Assessment date	Diseased plants	Expected runs	Standard deviation	Across rows		Within rows	
				Actual runs[a]	$Z(U)$[b]	Actual runs	$Z(U)$
Temple, cotton A ($n = 600$)[c]							
2 July	7	14.8	0.54	15	1.218	15	1.218
12 July	27	52.5	2.08	55	1.404	47	−2.430*
18 July	35	66.9	2.67	67	0.218	55	−4.271*
30 July	40	75.6	3.03	71	−1.375	63	−4.015*
13 August	230	284.6	11.57	261	−2.002*	215	−5.978*
Temple, soybean A ($n = 357$)							
2 July	3	6.9	0.28	7	1.914	7	1.914
12 July	64	106.0	5.54	105	−0.100	75	−5.514*
18 July	77	121.7	6.37	123	0.269	85	−5.692*
30 July	83	128.4	6.72	131	0.460	89	−5.784*
13 August	199	177.1	9.30	175	−0.177	107	−7.481*
Brandon, cotton ($n = 2,656$)							
19 June	139	264.4	5.10	221	−8.417*	207	−11,160*
26 June	365	630.6	12.21	461	−13.855*	439	−15.657*
3 July	675	1,007.9	19.53	631	−19.272*	595	−21.115*
17 July	1,163	1,308.5	25.37	743	−22.274*	692	−24.285*
31 July	1,332	1,328.9	25.76	777	−21.406*	660	−25.947*
7 August	1,562	1,287.7	24.96	705	−23.325*	606	−27.291*

[a] Values for actual runs were obtained by deriving an abstract lattice and assigning values of 0 or 1 for healthy and diseased plants, respectively.
[b] Value of the standardized normal deviate; randomness is rejected at $P = 0.05$ (shown as *), on a one-sided test, for $Z(U) = -1.64$.
[c] At the Temple location only, data for plots A of cotton and soybean were analyzed, see text. n = Number of entries in lattice.

TABLE 2. Results of spatial autocorrelation analysis for Phymatotrichum root rot, using the general cross product statistic r, of patterns of diseased plants of cotton at Temple and Brandon, TX

Assessment date	Observed[a]		Expected		Variance		Z[b]	
	Adj.[c]	Cont.[d]	Adj.	Cont.	Adj.	Cont.	Adj.	Cont.
Temple								
19 June	24	24	22.0	23.0	2.30	2.00	0.100	−0.04
26 June	104	86	110.5	111.6	24.06	22.66	1.124	5.16*
2 July	182	160	214.9	277.1	75.86	73.96	3.668*	6.51*
12 July	306	222	367.9	371.5	202.60	201.40	10.461*	10.47*
18 July	226	226	354.4	357.9	189.01	187.72	9.265*	9.55*
30 July	154	122	334.4	357.9	189.01	187.72	14.503*	17.14*
13 August	82	90	539.3	544.6	416.67	418.43	22.350*	22.17*
Brandon								
12 June	130	124	126	128	13.5	9.4	0.74	1.22
19 June	1,032	884	1,492	1,521	932.4	928.7	15.04*	20.88*
26 June	1,222	1,048	2,172	2,214	1,916.0	1,943.2	21.67*	26.42*
3 July	1,248	1,140	2,472	2,520	2,464.4	2,511.8	24.65*	27.53*
11 July	940	638	1,845	1,880	1,399.6	1,409.4	24.17*	33.08*
17 July	528	376	1,041	1,061	472.7	459.7	23.57*	31.93*
31 July	312	210	537	547	141.1	128.4	18.87*	29.70*
7 August	104	70	212	216	29.6	23.1	19.72*	30.26*

[a] Values for observed runs were obtained by dividing rows into 1-m segments and assigning values of 0 or 1 for segments in which there were no diseased plants or at least one diseased plant, respectively.
[b] Value of the standardized normal deviate; randomness is rejected at $P = 0.05$ (shown as *), on a one-sided test, for $Z = -1.64$.
[c] Adj. refers to the definition of spatial proximity as adjacent segments across rows.
[d] Cont. refers to the definition of spatial proximity as continguous segments within rows.

TABLE 3. Regression analysis of logit (p), where p is the relative frequency of transition, against x_1 (number of diseased contiguous segments) and x_2 (number of diseased adjacent segments) in cotton assessed for Phymatotrichum root rot at Brandon, TX

Date	Intercept[a]	Contiguous segment[b]	Adjacent segment[b]	Proportion of variance[c]
19 June	−1.56 (0.174)	2.25 (0.170)	1.48 (0.170)	0.99
26 June	−2.18 (0.102)	1.25 (0.230)	0.85 (0.206)	0.92
3 July	−1.82 (0.139)	0.78 (0.157)	0.83 (0.143)	0.94
10 July	−2.31 (0.090)	0.85 (0.193)	0.95 (0.183)	0.93
17 July	−2.98 (0.048)	0.77 (0.170)	0.76 (0.166)	0.92
7 August	−3.14 (0.041)	1.28 (0.389)	0.46 (0.370)	0.77
Combined	−2.00 (0.119)	0.74 (0.119)	0.61 (0.110)	0.95

[a] Values in parentheses are backtransformed values of the intercept.
[b] Values in parentheses are standard errors of coefficients (df = 8).
[c] Calculated as (total mean square − residual mean square)/total mean square.

during the early stage of the epidemic, but there was little difference later except at the last assessment; second, there was a trend for a decreasing intercept with time, indicating that the rate of appearance of diseased segments without diseased neighbors the previous week was not constant.

Results of the analyses using equation 2 are shown in Table 4. Including time in the equation significantly improved the fit of the equation. The relative contribution of within-row spread was higher than across rows. The analysis omitting time gave an equation very similar to the combined equation in Table 3.

Transition dynamics of run expansion. The transition frequencies are plotted for single-week transitions during early (26 June through 3 July, Fig. 8A), middle (11–18 July, Fig. 8B), and late (31 July through 7 August, Fig. 8C) stages of the epidemics and for the whole assessment period (Fig. 8D) by summing the totals for single-week transitions, then dividing by total transitions to obtain the correct frequencies. Most weekly transitions were made within the same length class, but there was extensive merging of short with long runs, shown by the extent of shading at the left of Figure 8A–D.

The actual numbers of runs observed to make a given transition during a 7-day period over the entire season are shown in Figure 9. The vertical axis (number of runs) was transformed to a square root scale for visual convenience. A regression analysis was undertaken to determine whether the nonzero transition frequencies could be predicted from the current and projected length classes; i.e., given that a run is currently in length class z_1, what is the relative frequency of transition to length class z_2 during the next 7 days? Data for the last sampling could only be used for z_2 variable. The relative frequency (a binary proportion) was weighted by the actual number of runs (Fig. 9) in the analyses. Two basic models were analyzed; in each case, the dependent variable was untransformed (y) or transformed with a range of transformations. The five unity values were excluded from the analysis. The independent variables in the first model took the form of an inverse quadratic with terms z_1^{-1}, z_2^{-1}, z_1^{-2}, z^{2-2}, and the product $(z_1z_2)^{-1}$. The single independent variable in the second model was either the difference $(z_2-z_1)^{-1}$, quotient $(z_2/z_1)^{-1}$, or product of these two terms. Results are shown in Table 5 for the untransformed relative frequency and the best transformation (note that $y \simeq -[\ln(1-y)]$ for small values of y). Each model resulted in equations accounting for a high proportion of the variance; the equation using the reciprocal of the difference gave the best fit of the single-variable equations. The probability (relative frequency) of a run expanding from one length class to another was inversely proportional to the difference in length between the two length classes.

DISCUSSION

The soilborne fungus *P. omnivorum* exemplifies many of the problems involved in describing and analyzing epidemics caused by root pathogens. It is relatively simple to assess and monitor the aboveground symptoms on plants in both time and space. The assessment is particularly simple with Phymatotrichum root rot because of the unambiguous symptomatology and rapid plant death. Conversely, it is exceedingly difficult to study, on scales of time and distance that can be related to the aboveground symptoms expression, the mechanisms (belowground) that lead to Phymatotrichum root rot epidemics. Insofar as epidemiology is essentially a compromise between studying a whole epidemic and the mechanisms generating the epidemic, no other area of epidemiology poses more challenges than studies of epidemics caused by root pathogens.

It is the scale and importance of plant-to-plant spread of Phymatotrichum root rot that is difficult to appraise realistically in a field context. It is relatively simple to assess growth of *P. omnivorum* through soil in greenhouse systems (45) and also in small plots or areas in the field; it would prove impossible on a realistic field scale as used in the studies described here. By combining information from the greenhouse and these field studies, it seems likely that plant-to-plant spread may be more important with *P. omnivorum* than that reported for most plant pathogens. First, the abundance of sclerotia in the soil is often low and clumped three-dimensionally (30), and yet extensive Phymatotrichum root rot development occurs in most years (21). Second, the rate of growth of *P. omnivorum* through soil in greenhouse systems (45) is larger than that reported for mycelial growth of most fungi (57). Third, although the between-season increase in the area of diseased plants increases radially, the within-season increase within these areas is characterized by within-row increase due to the formation of runs of diseased plants. This phenomenon was apparent from evaluation of spatial maps prepared in assessment of Phymatotrichum root rot (23–26,37–39,48,50); it is further supported by the data and quantitative analyses reported in this study. The evidence, however, is not direct until the means can be found to study strand growth and ramification through the soil in situ in field

TABLE 4. Regression analysis of logit (p), where p is the relative frequency of transition, against x_1 (number of diseased contiguous segments), x_2 (number of diseased adjacent segments), and t (time) in cotton dates assessed for Phymatotrichum root rot over all sampling dates at Brandon, TX

Regression	Intercept[a]	Contiguous segment[b]	Adjacent segment[b]	Time[b]	Proportion of variance[c]
Including time (t)	1.61 (0.167)	0.97 (0.124)	0.78 (0.116)	−0.26 (0.031)	0.82
Omitting time (t)	−2.01 (0.119)	0.80 (0.106)	0.57 (0.176)	···	0.55

[a] Values in parentheses are backtransformed values of the intercept.
[b] Values in parentheses are standard errors on coefficients (df = 43).
[c] Calculated as (total mean square − residual mean square)/total mean square.

TABLE 5. Regression analysis[a] of relative frequency (y) of a given transition with respect to the size classes of current (z_1) and next (z_2) run length of diseased plants in cotton assessed for Phymatotrichum root rot at Brandon, TX

	Model A[c]							Model B[c]		
Dependent variable[b]	Intercept	z_1^{-1}	z_2^{-1}	z_1^{-2}	z_2^{-2}	$(z_1z_2)^{-1}$	Proportion of variance	Intercept	$(z_2-z_1)^{-1}$	Proportion of variance[d]
y	0.21 (0.033)	−1.39 (0.142)	2.49 (0.107)	0.91 (0.093)	0.16 (0.044)	−1.61 (0.096)	0.98	0.054 (0.0107)	0.097 (0.0019)	0.97
$-\ln(1-y)$	0.21 (0.053)	−1.87 (0.228)	3.75 (0.171)	1.28 (0.150)	0.62 (0.070)	−2.73 (0.153)	0.99	0.027 (0.0248)	0.177 (0.0044)	0.95

[a] All regressions are based as $n = 32$ data points.
[b] Weighted by the total number of runs observed to make a given transition.
[c] Standard error of coefficients are shown in parentheses.
[d] Calculated as (total mean square − residual mean square)/total mean square. Value can validly be used to compare regression equations for the same dependent variable with different numbers of independent variables.

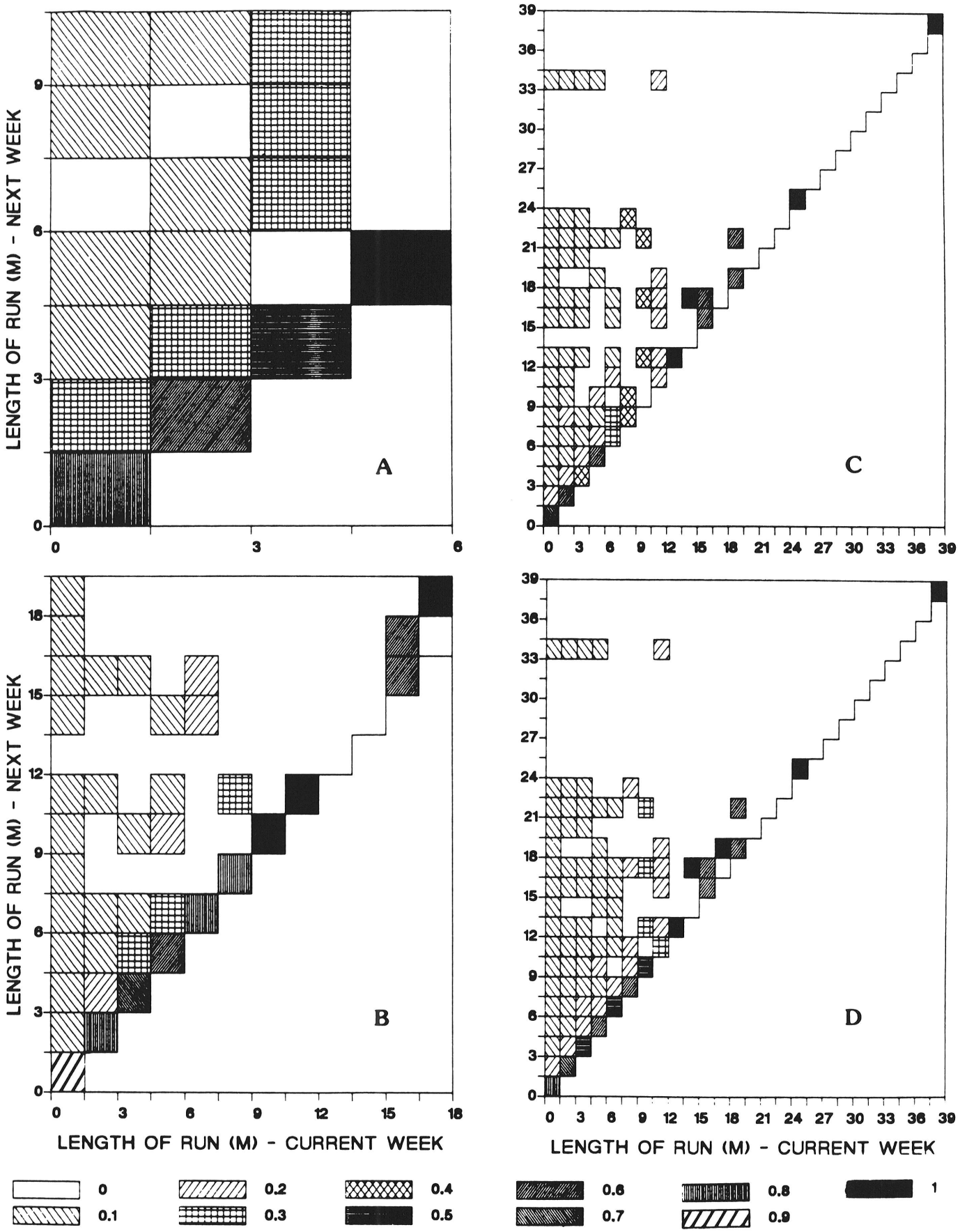

Fig. 8. Relative frequency of a run (sequence of diseased plants) making the transition from one size class (current week) to a larger size class (next week) in 1-wk intervals during **A,** early (26 June–3 July), **B,** middle (11–18 July), **C,** late (31 July–7 August), and **D,** over the complete period of the root rot epidemic in cotton at Brandon. Size classes are based on 1.5-m increments in length of run. Actual data points are represented at the bottom left corners of the shaded blocks. The areas in the lower right portions of (i.e., $z_2 < z_1$) represent impossible transitions; the "step" diagonal has been retained where necessary to indicate this. Blank areas in the upper left portions ($z_2 \geq z_1$) represent permissible transitions that were not observed. The solid-shaded areas represent instances where only one run was observed and made the transition indicated.

experiments of a scale comparable to that used to assess aboveground symptoms, where relatively large plot sizes are necessary to obtain reliable estimates of disease incidence (13). The use of recent technological advances, such as boroscope tubes, fiber optic technology, and video camera systems (55), is feasible in both laboratory and small-scale field systems and represents a useful technique to be exploited by epidemiologists. In the future, it may prove possible by the placement of such tubes in field plots to verify that run expansion arises from the spread of *P. omnivorum* strands along the rows of plants.

Some experimental investigations of the mechanisms underlying Phymatotrichum root rot epidemics have been made; most of these have involved fumigation or trenching experiments (22,25,26,38) and indicate that plant-to-plant spread does occur on a significant scale; these studies, however, severely interfere with the soil environment, and few have been designed directly to evaluate the relative importance of plant-to-plant spread. Plant density or seeding rate experiments can also be used to estimate the interplant distances over which *P. omnivorum* can grow and influence the development of root rot epidemics. Rogers (50) found that higher planting rates increased the percentage of plants with root rot. Koch et al (28) manipulated within-row density and between-row spacing in large (10 m^2) field plots and found that doubling row spacing had no effect on estimated parameters of disease progress where these included initial disease, rate of epidemic increase, disease asymptote, and the area under the progress curve. By means of simple calculations, they concluded that the interplant distance inhibiting epidemic development of Phymatotrichum root rot in one particular year at the Temple site lay in the range 20–69 cm.

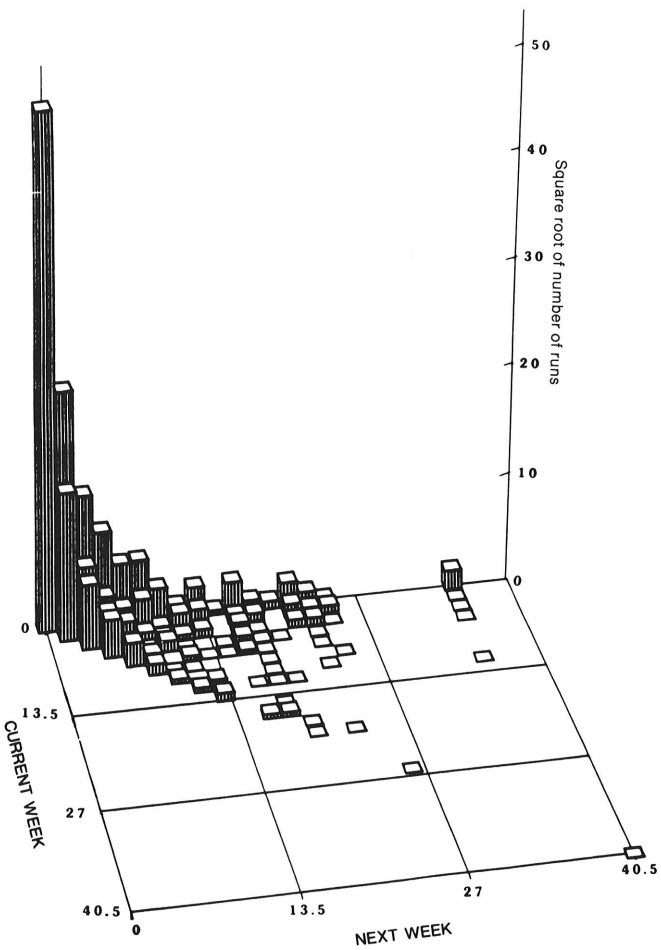

Fig. 9. Number of runs (sequences of diseased plants) observed to make the transition from one size class (current week) to a larger size class (next week) during 1-wk periods of the root rot epidemic in cotton at Brandon. Size classes are based on 1.5-m increments in length of run. Labels against size classes refer to actual length of run (m).

The difficulties experienced in designing and conducting field experiments that combine both aboveground assessment of symptoms and belowground observation of mechanisms indicates that mathematical models should be of great value in exploring the consequences of competing hypotheses of the spatial dynamics of Phymatotrichum root rot in row crops and in designing appropriate experiments. Two modeling approaches (M. J. Jeger, *unpublished*) have been taken and are outlined to pose the nature of the problem and to relate them to the data reported in this paper.

First, a theoretical approach can be taken in which qualitative analysis is used to extract the essential dynamic behavior of the system (20). Note that the total number of plants diseased (y) can be expressed as the product of the number of runs (x) and the mean number of diseased plants per run (n). Hence,

$$y = xn, \tag{3}$$

from which, using the product rule,

$$dy/dt = x\, dn/dt + n\, dx/dt. \tag{4}$$

It is then necessary to develop differential equations for x and for n to develop the model further.

The rate of change in x is given by increases in the number of runs less decreases resulting from the merging of previous runs. The increases in runs are given by those diseased plants that appear for the first time either singly or as more than one plant in new runs. These can be written as a function of time and described empirically from data such as Figures 2B, 6B, and 7B or by using probability functions. A major problem arises in determining an analytical expression for the decreases in runs resulting from mergings; these are dependent on both the number of runs (x) and the total number of diseased plants.

The rate of change in n is the rate of change of mean number of plants per run. If there were only one run to consider, and because expansion can only occur from the two extreme plants, then the rate would be constant (as observed at Brandon, Fig. 2C). With new runs appearing and merging, however, there are severe problems in specifying the rates of increase in either mean numbers of plants per run or the mean rate of increase per run.

An alternative to the theoretical approach is to simulate disease progress on a spatially explicit two-dimensional map and to evaluate the consequences of competing mechanisms of increase on the spatio-temporal patterns of diseased plants. This type of approach, in a simplified form, has been taken with virus diseases (14,16). For example, two scenarios could be constructed in which: 1) disease increase is due only to encounter of a developing root system with spatially distributed inoculum in soil; 2) disease increase is due to the first scenario and also to growth of fungal strands through soil. Using Monte-Carlo simulation techniques, the probability distributions for defined model parameters are then used for comparison with estimated parameters.

From a practical standpoint, there is also a lack of quantitative methods to describe spatial dynamics of root disease epidemics. There are many methods available for describing the temporal progress of an epidemic (32,33), but these have largely ignored spatial considerations (18,19,41). The nearest neighbor type of analysis used in this paper offers some potential (4,19, Besag in Discussion of Mollison [42]) but deals with spatial considerations implicitly rather than explicitly. There are many techniques available for examining the spatial patterns of disease at a given time, but these only offer a static "snapshot" of the epidemic. Combined space-time models are needed to describe the spatial dynamics of disease. Such models may be cumbersome (56), but their development, simplification, and use should be explored further for plant disease epidemics.

LITERATURE CITED

1. Alderman, S. C., and Hine, R. B. 1982. Vertical distribution in soil and induction of disease by strands of *Phymatotrichum omnivorum*. Phytopathology 72:409-412.

2. Alderman, S. C., and Stowell, L. J. 1986. Strand ontogeny in *Phymatotrichum omnivorum*. Trans. Br. Mycol. Soc. 86:207-211.
3. Anonymous. 1984. 1983 Texas Field Crop Statistics. Bull. 221, Tex. Dep. Agric./U.S. Dep. Agric. 96 pp.
4. Bartlett, M. S. 1975. The Statistical Analysis of Spatial Pattern. Chapman and Hall, London.
5. Campbell, C. L., Jacobi, W. R., Powell, N. T., and Main, C. E. 1984. Analysis of disease progression and the randomness of occurrence of infected plants during tobacco black shank epidemiology. Phytopathology 74:230-235.
6. Campbell, C. L., and Noe, J. P. 1985. The spatial analysis of soilborne pathogens and root diseases. Annu. Rev. Phytopathol. 23:129-148.
7. Crowe, F. W., Hall, D. H., Greathead, A. S., and Baghott, K. G. 1980. Inoculum density of *Sclerotium cepivorum* and the incidence of white rot of onion and garlic. Phytopathology 70:64-69.
8. Dale, W. T. 1953. Further notes on the spread of virus in a field of clonal cacao in Trinidad. Pages 130-131 in: Cocoa Research 1945–1951. Imperial College of Tropical Agriculture, Trinidad.
9. Dillard, H. R., and Grogan, R. G. 1985. Relationship between sclerotial spatial pattern and density of *Sclerotina minor* and the incidence of lettuce drop. Phytopathology 75:90-94.
10. Eaton, E. D., and King, C. J. 1934. A study of the cotton root-rot fungus (*Phymatotrichum omnivorum*) in the soil by the cholodny method. J. Agric. Res. 49:1093-1113.
11. El-Zik, K. M., and Frisbie, R. E. 1985. Integrated crop management systems for pest control. Pages 21-122 in: CRC Handbook of Natural Pesticides: Methods. Vol. 1. Theory, Practice and Detection. N. Bushan Mandavia, ed. CRC Press, Boca Raton, FL.
12. Entwistle, A. R., and Munasinghe, H. L. 1977. White rot disease of onions: Spread of white rot in the row. Page 97 in: Report of the National Vegetable Research Station, Wellesbourne for 1976. Wellesbourne, UK.
13. Gerik, T. J., Rush, C. M., and Jeger, M. J. 1985. Optimizing plot size for field studies of Phymatotrichum root rot of cotton. Phytopathology 75:240-243.
14. Gibbs, A. 1983. A simple convolution method for describing or comparing the distributions of virus-affected plants in a plant community. Pages 39-50 in: Plant Virus Epidemiology: The Spread and Control of Insect-borne Viruses. R. T. Plumb and J. M. Thresh, eds. Blackwell Scientific Publications, Oxford.
15. Gitaitis, R. D., Stall, R. E., and Strandberg, J. O. 1978. Dissemination and survival of *Pseudomonas alboprecipitans* ascertained by disease distribution. Phytopathology 68:227-231.
16. Gray, S. M., Moyer, J. W., and Bloomfield, P. 1986. Two-dimensional distance class model for quantitative description of virus-infected plant distribution lattices. Phytopathology 76:243-248.
17. Huang, H. C., and Hoes, J. A. 1980. Importance of plant spacing and sclerotial position to development of sclerotinia wilt of sunflower. Plant Dis. 64:81-84.
18. Jeger, M. J. 1983. Analyzing epidemics in time and space. Plant Pathol. 32:5-11.
19. Jeger, M. J. 1985. Models of focus expansion in disease epidemics. Pages 279-288 in: The Movement and Dispersal of Agriculturally Important Biotic Agents. D. R. MacKenzie, C. S. Barfield, G. C. Kennedy, and R. D. Berger, eds. Claitor's Publishing Division, Baton Rouge.
20. Jeger, M. J. 1986. The potential of analytic compared with simulation approaches to modeling in plant disease epidemiology. Pages 255-281 in: Plant Disease Epidemiology. Vol. 1. Population Dynamics and Management. K. J. Leonard and W. E. Fry, eds. Macmillan, New York. 372 pp.
21. Jeger, M. J., and Lyda, S. D. 1986. Epidemics of root rot (*Phymatotrichum omnivorum*) in cotton, environmental correlates of final incidence and forecasting criteria. Ann. Appl. Biol. 109:523-534.
22. King, C. J. 1923. Habits of the cotton root rot fungus. J. Agric. Res. 26:405-418.
23. King, C. J., Hope, C., and Eaton, E. D. 1935. Some microbial activities affected in minimal control of cotton root rot. J. Agric. Res. 49:1093-1113.
24. King, C. J., and Loomis, H. F. 1926. Experiments on the control of cotton root rot in Arizona. J. Agric. Res. 32:297-310.
25. King, C. J., and Loomis, H. F. 1929. Cotton root rot investigations in Arizona. J. Agric. Res. 39:199-221.
26. King, C. J., and Loomis, H. F. 1929. Further studies of cotton root rot in Arizona with a description of a sclerotium stage of the fungus. J. Agric. Res. 39:641-676.
27. King, C. J., Loomis, H. F., and Hope, C. 1931. Studies on sclerotia and mycelial strands of the cotton root-rot fungus. J. Agric. Res. 42:827-840.
28. Koch, D. O., Jeger, M. J., Gerik, T. J., and Kenerley, C. M. 1987. Effects of plant density on progress of Phymatotrichum root rot in cotton. Phytopathology 77:1645-1650.
29. Lyda, S. D. 1978. Ecology of *Phymatotrichum omnivorum*. Annu. Rev. Phytopathol. 16:193-209.
30. Lyda, S. D. 1984. Vertical and horizontal distribution of *Phymatotrichum sclerotia* in Texas soils. (Abstr.) Phytopathology 74:814.
31. MacNish, G. C. 1985. Mapping rhizoctonia patch in consecutive cereal crops in Western Australia. Plant Pathol. 34:165-174.
32. Madden, L. V. 1980. Quantification of disease progression. Prot. Ecol. 2:159-176.
33. Madden, L. V. 1986. Statistical analysis and comparison of disease progress curves. Pages 55-84 in: Plant Disease Epidemiology. Vol. 1. Population Dynamics and Management. K. Leonard and W. E. Fry, eds. Macmillan, New York. 372 pp.
34. Madden, L. V., Louie, R., Abt, J. J., and Knoke, J. K. 1982. Evaluation of tests for randomness of infected plants. Phytopathology 72:195-198.
35. Madden, L. V., Louie, R., and Knoke, J. K. 1987. Temporal and spatial analysis of maize dwarf mosaic epidemics. Phytopathology 77:148-156.
36. Marois, J. J., and Adams, P. B. 1985. Frequency distribution analyses of lettuce drop caused by *Sclerotinia minor*. Phytopathology 75:957-961.
37. McNamara, H. C. 1926. Behavior of cotton root rot at Greenville, Texas, including an experiment with clean fallows. J. Agric. Res. 32:17-24.
38. McNamara, H. C., and Hooton, D. R. 1929. Studies of cotton root rot at Greenville, Texas. U.S. Dep. Agric. Circ. 85. 16 pp.
39. McNamara, H. C., Hooton, D. R., and Porter, D. D. 1931. Cycles of growth in cotton root rot at Greenville, Texas. U.S. Dep. Agric. Circ. 173. 17 pp.
40. McNamara, H. C., Webster, R. E., and Gunn, K. C. 1933. Persistent strands of the root rot fungus in Texas. Science 7:510-511.
41. Minogue, K. P., and Fry, W. E. 1983. Models for the spread of disease: Model description. Phytopathology 73:1168-1173.
42. Mollison, D. 1977. Spatial contact models for ecological and epidemic spread. J. R. Stat. Soc. B, 39:283-326.
43. Nicot, P. C., Rouse, D. I., and Yandell, B. S. 1984. Comparison of statistical methods for studying spatial patterns of soilborne plant pathogens in the field. Phytopathology 74:1399-1402.
44. Percy, R. G. 1983. Potential range of *Phymatotrichum omnivorum* as determined by edaphic factors. Plant Dis. 67:981-983.
45. Percy, R. G., and Rush, C. M. 1985. Evaluation of four upland cotton genotypes for a rate-limiting resistance to Phymatotrichum root rot. Phytopathology 75:463-466.
46. Punja, Z. K. 1985. The biology, ecology and control of *Sclerotium rolfsii*. Annu. Rev. Phytopathol. 23:97-127.
47. Punja, Z. K. 1986. Progression of root rot of processing carrots due to *Sclerotium rolfsii* and the relationship of disease incidence to inoculum density. Can. J. Plant Pathol. 8:297-304.
48. Ratliffe, G. T. 1934. Cotton root rot as affected by crop rotation and tillage at San Antonio, Tex. U.S. Dep. Agric. Tech. Bull. 31 pp.
49. Rea, H. E. 1939. The control of cotton root rot in the Blackland region of Texas. Tex. Agric. Exp. Stn. Bull. 573. 36 pp.
50. Rogers, C. H. 1942. Cotton root rot studies with special reference to sclerotia, cover crops rotations, tillage, seeding rates, soil, fungicides, and effects on seed quality. Tex. Agric. Exp. Stn. Bull. 614.
51. Schuh, W., Frederiksen, R. A., and Jeger, M. J. 1986. Analysis of spatial patterns in sorghum downy mildew with Morisita's index of dispersion. Phytopathology 76:446-450.
52. Shew, B. B., Beute, M. K., and Campbell, C. L. 1984. Spatial pattern of southern stem rot caused by *Sclerotium rolfsii* in six North Carolina peanut fields. Phytopathology 74:730-735.
53. Streets, R. B., and Bloss, H. E. 1973. Phymatotrichum root rot. Monogr. 8. Am. Phytopathol. Soc., St. Paul, MN. 38 pp.
54. Taubenhaus, J. J., and Killough, D. T. 1923. Texas root rot of cotton and methods of its control. Tex. Agric. Exp. Stn. Bull. 307. 98 pp.
55. Upchurch, D. R., and Ritchie, J. T. 1983. Root observations using a video recording system in mini-rhizotrons. Agron. J. 75:1005-1015.
56. Upton, G., and Fingleton, B. 1985. Spatial Data Analysis by Example. Vol. 1. Point Pattern and Quantitative Data. John Wiley & Sons, Chichester. 410 pp.
57. Wallace, H. R. 1978. Dispersal in time and space: Soil pathogens. Pages 181-202 in: Plant Disease. An Advanced Treatise. Vol. 2. How Disease Develops in Populations J. G. Horsfall and E. B. Cowling, eds. Academic Press, New York.
58. Wehrle, V. M., and Ogilvie, L. 1952. Spread of take-all from infected wheat plants. Plant Pathol. 5:106-107.